

Hydro/Solvothermal Synthesis and Structures of New Zinc Phosphates of Varying Dimensionality

Srinivasan Natarajan*

Framework Solids Laboratory, Chemistry and Physics of Materials Unit, Jawaharlal Nehru Centre for Advanced Scientific Research, Jakkur P.O., Bangalore 560 064, India

Received June 7, 2002

Hydro/solvothermal reactions of ZnO, HCl, H₃PO₄, 1,4-diazacycloheptane (homopiperazine), and H₂O under a variety of conditions yielded three new organic–inorganic hybrid materials, [C₅N₂H₁₄][Zn(HPO₄)₂] \cdot xH₂O ($x = \sim 0.46$), **I**, [C₅N₂H₁₄][Zn₃(H₂O)(PO₄)₂(HPO₄)], **II**, and [C₅N₂H₁₄][Zn₂(HPO₄)₃] \cdot H₂O, **III**. While **I** has a one-dimensional structure, **II** possesses a two-dimensional layered structure, and **III** has a three-dimensional structure closely related to the ABW zeolitic architecture. All the compounds consist of vertex linking of ZnO₄, PO₄, and HPO₄ tetrahedral units. The fundamental building unit, single four-membered ring (S4R), is present in all the cases, and the observed differences in their structures result from variations in the connectivity between the S4R units. Thus **I** has a corner-shared S4R forming an infinite one-dimensional chain, **II** has two corner-shared chains fused through a 3-coordinated oxygen atom forming a strip and a layer with eight-membered apertures, and **III** has S4R units connected via oxygen atoms to give rise to channels bound by eight T atoms (T = Zn, P) in all crystallographic directions. Crystal data: **I**, monoclinic, space group = $P2_1/n$ (No. 14), $a = 8.6053(3)$ Å, $b = 13.7129(5)$ Å, $c = 10.8184(4)$ Å, $\beta = 97.946(1)^\circ$, $V = 1264.35(8)$ Å³, $Z = 4$; **II**, monoclinic, space group = $P2_1/c$ (No. 14), $a = 11.1029(1)$ Å, $b = 17.5531(4)$ Å, $c = 8.2651(2)$ Å, $\beta = 97.922(2)^\circ$, $V = 1595.42(5)$ Å³, $Z = 4$; **III**, monoclinic, space group = $P2_1$ (No. 4), $a = 8.0310(2)$ Å, $b = 10.2475(3)$ Å, $c = 10.570(3)$ Å, $\beta = 109.651(1)^\circ$, $V = 819.24(3)$ Å³, $Z = 2$.

Introduction

The research in the area of solids with open architecture continues to be interesting for their many potential applications in the area of catalysis, sorption, and separation processes. Though aluminosilicate zeolites and aluminophosphates are the most widely studied class of solids, open-framework metal phosphates also assumed an important position.¹ Of these, zinc phosphates with open architectures are interesting due to the fact that the total charges associated with them (+2 and +5) are similar to those of the aluminosilicates (+3 and +4), resulting in zinc phosphates with zeolitic structures.^{2–7} Of the many zinc phosphates,

ND-1 is important for the extra-large 24-membered one-dimensional channels.⁸ In addition to the above, zinc phosphates with zero-,^{9–11} one-,^{12–16} two-,^{17–21} and three-dimensional^{22–38} structures have also been prepared and characterized. Based on the observation of the structural similarities between the various zinc phosphates, an *aufbau* principle of building higher-dimensional structures from that of the lower-dimensional ones has also been suggested.^{39,40}

Open-framework phosphates are, in general, prepared by employing hydro/solvothermal methods in the presence of an organic amine. The amine molecule generally occupies cavities and channels and in some cases can be removed by

* Corresponding author. E-mail: raj@jncasr.ac.in. FAX: +91-80-846-2766; +91-80-856-6581.

- (1) Cheetham, A. K.; Ferey, G.; Loiseau, T. *Angew. Chem., Int. Ed.* **1999**, *39*, 3268 and references therein.
- (2) Feng, P.; Bu, X.; Stucky, G. D. *Angew. Chem., Int. Ed. Engl.* **1995**, *34*, 1745.
- (3) Gier, T. E.; Stucky, G. D. *Nature* **1991**, *349*, 508.
- (4) Ng, H. Y.; Harrison, W. T. A. *Microporous Mesoporous Mater.* **2001**, *50*, 187.
- (5) Neeraj, S.; Natarajan, S. *J. Phys. Chem. Solids* **2001**, *62*, 1499.
- (6) Harrison, W. T. A.; Gier, T. E.; Moran, K. L.; Nicol, J. M.; Eckert, H.; Stucky, G. D. *Chem. Mater.* **1991**, *3*, 27.

(7) Nenoff, T. M.; Harrison, W. T. A.; Gier, T. E.; Stucky, G. D. *J. Am. Chem. Soc.* **1991**, *113*, 78.

(8) Yang, G.-Y.; Sevov, S. C. *J. Am. Chem. Soc.* **1999**, *121*, 8389.

(9) Neeraj, S.; Natarajan, S.; Rao, C. N. R. *J. Solid State Chem.* **2000**, *150*, 417.

(10) Ayi, A. A.; Choudhury, A.; Natarajan, S.; Neeraj, S.; Rao, C. N. R. *J. Mater. Chem.* **2001**, *11*, 1181.

(11) Harrison, W. T. A.; Hannonman, L. *J. Solid State Chem.* **1997**, *131*, 363.

(12) Chavaz, A. V.; Nenoff, T. M.; Hannonman, L.; Harrison, W. T. A. *J. Solid State Chem.* **1999**, *147*, 584.

(13) Rao, C. N. R.; Natarajan, S.; Neeraj, S. *J. Am. Chem. Soc.* **2000**, *122*, 2810.

postsynthesis treatments such as calcination, acid-leaching, etc. Predominantly the amine molecules are protonated during the hydrothermal reaction, and this protonation helps in the charge balance of the inorganic framework. Though some understanding has been achieved of the formation of open-framework structures,^{39–45} the synthesis of these solids still retains the exploratory component. In zinc phosphates, it has been observed that the use of linear diamines or polyamines seems to be more efficient than the use of monoamines in directing the formation of materials with open architectures. Of the cyclic amines, diaminocyclohexane (DACH),⁸ piperazine (1,3-diazacyclohexane),^{2,13} and 1,4-diazabicyclo[2.2.2]octane (DABCO)^{24,25} have been used extensively, resulting in the formation of new zinc phosphates of varying dimensionalities. In a continuing theme of research aimed at producing new materials employing cyclic amines, we have been investigating the formation of new zinc phosphates in the presence of 1,4-diazacycloheptane (homopiperazine, H-PIP). Our efforts were indeed successful,

and we have now isolated three new zinc phosphates, $[C_5N_2H_{14}][Zn(HPO_4)_2] \cdot xH_2O$ ($x = \sim 0.46$), **I**, $[C_5N_2H_{14}][Zn_3(H_2O)(PO_4)_2(HPO_4)]$, **II**, and $[C_5N_2H_{14}][Zn_2(HPO_4)_3] \cdot H_2O$, **III**. The structures of **I–III** consists of ZnO_4 , PO_4 , and HPO_4 tetrahedral units linked through their vertices giving rise to one-, two-, and three-dimensional structures. While **I** has a corner-shared single four-membered ring (S4R) forming infinite one-dimensional chains, **II** has two corner-shared chains fused through a 3-coordinated oxygen atom forming a strip and a layer with eight-membered apertures and **III** has S4R units connected via oxygen atoms to give rise to channels bound by eight T atoms (T = Zn, P) in all crystallographic directions and is closely related to the ABW-zeolitic architecture.^{46,47} In this paper, the synthesis, structure, and characterization of **I–III** are presented.

Experimental Section

Synthesis and Initial Characterization. Compounds **I–III** were synthesized under hydrothermal conditions using a mixture of THF and water as solvents in the presence of homopiperazine (H-PIP). In a typical synthesis, for **I**, 0.20 g of ZnO was dispersed in a mixture of 4 mL of THF and 3 mL of H₂O. To this were added 0.41 mL of hydrochloric acid (35%), 0.92 mL of phosphoric acid (88%), and 0.15 mL of acetic acid with constant stirring. Finally, 1.0 g of H-PIP was added and the mixture was homogenized for 30 min at room temperature. The final reaction mixture with the composition ZnO:2HCl:3H₃PO₄:4H-PIP:CH₃COOH:(19.5THF + 66.6H₂O) was sealed in a 23 mL PTFE-lined stainless steel autoclave and heated at 75 °C for 72 h. The initial pH of the reaction mixture was found to be ~ 3 . The resulting product contained large quantities of colorless rodlike crystals, suitable for single-crystal X-ray diffraction, and was vacuum filtered, washed with deionized water, and dried under ambient conditions. The yield of **I** was about 80% based on Zn. For **II** and **III**, a synthesis mixture of the composition 2ZnO:4HCl:4H₃PO₄:6H-PIP:CH₃COOH:(19.5THF + 66.6H₂O) was employed but heated at different temperatures. Thus, for **II**, the synthesis mixture was heated at 75 °C for 72 h, and for **III**, at 75 °C for 72 h, followed by at 150 °C for 24 h and at 180 °C for 24 h, respectively. The resulting product, in both cases, contained only single crystals (colorless plates for **II** and colorless thick hexagons for **III**), which were removed by vacuum filtration, washed with deionized water, and dried under ambient conditions. The initial pH of the reaction mixture in both cases was close to ~ 8 . The yields of **II** and **III** were about 90% and 60%, respectively. Our efforts to prepare **I–III** in pure aqueous medium, however, were not successful. An EDAX analysis on many single crystals indicated a Zn/P ratio of 1:2 for **I**, 1:1 for **II** and 1:1.5 for **III**, consistent with the single-crystal X-ray analysis. Elemental analysis results of the bulk product are also consistent with the stoichiometry. Anal. Calcd for **I**: C, 16.24; H, 4.87; N, 7.58. Found: C, 16.18; H, 4.92; N, 7.54. Calcd for **II**: C, 9.96; H, 2.82; N, 4.65. Found: C, 9.91; H, 2.76; N, 4.59. Calcd for **III**: C, 11.13; H, 3.53; N, 5.20. Found: C, 10.98; H, 3.58; N, 5.27.

The initial characterization was carried out using powder X-ray diffraction (XRD), thermogravimetric analysis (TGA), and infrared spectroscopy. The powder XRD pattern indicated that the products were new materials; the patterns were entirely consistent with the structures determined using the single-crystal X-ray diffraction. A

- (14) Chidambaram, D.; Neeraj, S.; Natarajan, S.; Rao, C. N. R. *J. Solid State Chem.* **1999**, *147*, 154.
- (15) Harrison, W. T. A.; Bircsak, Z.; Hannoman, L.; Zhang, Z. J. *J. Solid State Chem.* **1998**, *136*, 93.
- (16) Ayi, A. A.; Neeraj, S.; Choudhury, A.; Natarajan, S.; Rao, C. N. R. *J. Phys. Chem. Solids* **2001**, *62*, 1481.
- (17) Neeraj, S.; Natarajan, S.; Rao, C. N. R. *Chem. Mater.* **1999**, *11*, 1390.
- (18) Neeraj, S.; Natarajan, S. *Int. J. Inorg. Mater.* **1999**, *1*, 317.
- (19) Neeraj, S.; Natarajan, S. *Cryst. Growth Des.* **2001**, *1*, 491.
- (20) Choudhury, A.; Natarajan, S.; Rao, C. N. R. *J. Solid State Chem.* **2001**, *157*, 110.
- (21) Harrison, W. T. A.; Phillips, M. L. F.; Clegg, W.; Teat, S. J. *J. Solid State Chem.* **1999**, *148*, 433 and references therein.
- (22) Song, T.; Hurshouse, M. B.; Chen, J.; Xu, J.; Malik, K. M. A.; Jones, R. H.; Xu, R.; Thomas, J. M. *Adv. Mater.* **1994**, *6*, 679.
- (23) Liu, Y.; Na, L.; Zhu, G.; Xio, F.-S.; Pang, W.; Xu, R. *J. Solid State Chem.* **2000**, *149*, 107.
- (24) Harrison, W. T. A.; Martin, T. E.; Gier, T. E.; Stucky, G. D. *J. Mater. Chem.* **1992**, *2*, 1127.
- (25) Natarajan, S.; Neeraj, S.; Rao, C. N. R. *Solid State Sci.* **2000**, *2*, 89.
- (26) Harrison, W. T. A.; Nenoff, T. M.; Gier, T. E.; Stucky, G. D. *Inorg. Chem.* **1992**, *31*, 5395.
- (27) Feng, P.; Bu, X.; Stucky, G. D. *J. Solid State Chem.* **1996**, *125*, 243.
- (28) Bu, X.; Feng, P.; Gier, T. E.; Stucky, G. D. *Zeolites* **1997**, *19*, 2000.
- (29) Broach, R. W.; Bedard, R. L.; Song, S. G.; Pluth, J. J.; Bram, A.; Riekel, C.; Weber, H.-P. *Chem. Mater.* **1999**, *11*, 2076.
- (30) Harrison, W. T. A.; Nenoff, T. M.; Gier, T. E.; Stucky, G. D. *Inorg. Chem.* **1993**, *32*, 2437.
- (31) Harrison, W. T. A.; Phillips, M. L. F. *Chem. Mater.* **1997**, *9*, 1837.
- (32) Harrison, W. T. A.; Hannooman, L. *Angew. Chem., Int. Ed. Engl.* **1997**, *36*, 640.
- (33) Harrison, W. T. A.; Dussak, L. L.; Jacobson, A. J. *J. Solid State Chem.* **1996**, *125*, 134.
- (34) Kongshaug, K. O.; Fjellvag, H.; Lillerud, K. P. *J. Mater. Chem.* **1999**, *9*, 3119.
- (35) Chidambaram, D.; Natarajan, S. *Mater. Res. Bull.* **1998**, *33*, 1275.
- (36) Neeraj, S.; Natarajan, S.; Rao, C. N. R. *Chem. Commun.* **1999**, 165.
- (37) Choudhury, A.; Natarajan, S.; Rao, C. N. R. *Inorg. Chem.* **2000**, *39*, 4295.
- (38) Neeraj, S.; Natarajan, S. *Chem. Mater.* **2000**, *11*, 2735.
- (39) Rao, C. N. R.; Natarajan, S.; Choudhury, A.; Neeraj, S.; Ayi, A. A. *Acc. Chem. Res.* **2001**, *34*, 80.
- (40) Rao, C. N. R.; Natarajan, S.; Choudhury, A.; Neeraj, S.; Vaidyanathan, R. *Acta Crystallogr.* **2002**, *B57*, 1.
- (41) Oliver, S.; Kuperman, A.; Ozin, G. A. *Angew. Chem., Int. Ed.* **1998**, *37*, 46.
- (42) Ferey, G. C. R. *Acad. Sci. Paris, Ser. IIC* **1998**, 1.
- (43) Walton, R. I.; Millange, F.; Le Bail, A.; Loiseau, T.; Serre, C.; O'Hare, D.; Ferey, G. *Chem. Commun.* **2000**, 203.
- (44) Walton, R. I.; Loiseau, T.; O'Hare, D.; Ferey, G. *Chem. Mater.* **2000**, *12*, 1977.
- (45) Walton, R. I.; Norquist, A. J.; Neeraj, S.; Natarajan, S.; Rao, C. N. R.; O'Hare, D. *Chem. Commun.* **2001**, 1990 and the references therein.

(46) Barrer, R. M.; White, E. A. D. *J. Chem. Soc.* **1951**, 1267.

(47) Baerlocher, Ch.; Meier, W. M.; Olson, D. H., Eds. *Atlas of zeolitic structure types*; Elsevier: London, 2001.

least-squares fit of the powder XRD (Cu K α radiation) lines, using the *hkl* indices generated from single-crystal X-ray data, gave the following cells: for **I**, $a = 8.632(2)$ Å, $b = 13.647(2)$ Å, $c = 10.789(4)$ Å, $\beta = 97.65(1)^\circ$; for **II**, $a = 11.119(6)$ Å, $b = 17.491(7)$ Å, $c = 8.195(3)$ Å, $\beta = 96.88(2)^\circ$; and for **III**, $a = 8.020(2)$ Å, $b = 10.212(5)$ Å, $c = 10.623(2)$ Å, $\beta = 109.74(2)^\circ$. These results are in reasonable agreement with those determined using the single-crystal XRD.

Thermogravimetric analysis (TGA) of compounds **I–III** were carried out in oxygen atmosphere in the range between 25 and 700 °C. For **I**, the release of amine from the structure was observed to be highly exothermic, resulting in the sample being thrown out of the crucible. To overcome this experimental handicap a very slow heating rate of 1 °C min⁻¹ was employed, and for **II** and **III**, a heating rate of 5 °C/min was used. The TGA studies indicate that the weight loss occurs in two steps with a broad tail for **I**, in one sharp step followed by a tail for **II**, and in three steps for **III**. The first mass loss of 5.84% around 150 °C corresponds well with the loss of adsorbed and extraframework water molecules (calcd 4.78%), and the next mass loss of 35.3% for the next step with the tail in the range 350–500 °C corresponds to the loss of the amine and the condensation of terminal P–OH groups (calcd 36.2%). In the case of **II**, the sharp mass at 350 °C followed by a tail of 18.2% in the 400–600 °C range corresponds to the loss of the amine and condensation of P–OH groups (calcd 19.8%). In the case of **III**, a mass loss of 4.2% around 150 °C corresponds to the loss of the adsorbed and extraframework water molecules (calcd 3.4%), a second mass of 17.7% in the range 325–400 °C corresponds to the loss of the amine (calcd 18.9%), and finally a broad mass loss of 9% in the range 475–600 °C corresponds to the condensation of the P–OH groups (calcd 9.5%). In all cases, the loss of the amine molecule resulted in the collapse of the framework structure, leading to the formation of largely amorphous weakly diffracting materials (XRD) that correspond to dense zinc phosphate phases; Zn₃(PO₄)₂ [JCPDS: 30-1489] for **I** and **III**, and Zn₂P₂O₇ [JCPDS: 34-1275] for **II**.

Infrared (IR) spectra of **I–III** were recorded in the range 400–4000 cm⁻¹ using the KBr pellet method. The IR spectra of all three compounds showed typical peaks, with very little differences between the spectra. Strong absorption bands for N–H and O–H bending and stretching vibrations are observed at 3012, 1620, and 1458 cm⁻¹ for all of the compounds. A strong band at 3647 cm⁻¹ has been observed for **I** and **III**, corresponding to the extraframework water molecule. In addition, bands in the 1275–1578 cm⁻¹ range are attributed to C–C stretching and those at 1080 cm⁻¹ to C–N stretching.

Single-Crystal Structure Determination. A suitable colorless single crystal of each compound was carefully selected under a polarizing microscope and glued to a thin glass fiber with cyanoacrylate (superglue) adhesive. Crystal structure determination by X-ray diffraction was performed on a Siemens SMART-CCD diffractometer equipped with a normal focus, 2.4 kW sealed-tube X-ray source (Mo K α radiation, $\lambda = 0.71073$ Å) operating at 50 kV and 40 mA. A hemisphere of intensity data were collected at room temperature in 1321 frames with ω scans (width of 0.30° and exposure time of 10 s per frame) in the 2θ range 3–46.5°. Pertinent experimental details for the structure determinations of **I–III** are presented in Table 1.

An absorption correction based on symmetry equivalent reflections was applied using the SADABS program.⁴⁸ Other effects, such

Table 1. Crystal Data and Structure Refinement Parameters for [C₅N₂H₁₄][Zn(HPO₄)₂] \cdot *x*H₂O ($x = \sim 0.46$), **I**, [C₅N₂H₁₄][Zn₃(H₂O)(PO₄)₂(HPO₄)], **II**, and [C₅N₂H₁₄][Zn₂(HPO₄)₃] \cdot H₂O, **III**

	I	II	III
empirical formula	C ₅ H ₁₈ N ₂ O ₉ P ₂ Zn	C ₅ H ₁₇ N ₂ O ₁₃ P ₃ Zn ₃	C ₅ H ₁₉ N ₂ O ₁₃ P ₃ Zn ₂
fw	376.52	602.23	538.87
<i>T</i> (K)	298	298	298
space group	<i>P</i> 2 ₁ / <i>n</i> (No. 14)	<i>P</i> 2 ₁ / <i>c</i> (No. 14)	<i>P</i> 2 ₁ (No. 4)
<i>a</i> /Å	8.6053(3)	11.1029(1)	8.0310(2)
<i>b</i> /Å	13.7129(5)	17.5531(4)	10.2475(3)
<i>c</i> /Å	10.8184(4)	8.2651(2)	10.570(3)
β /deg	97.946(1)	97.922(2)	109.651(1)
<i>V</i> /Å ³	1264.35(8)	1595.42(5)	2097.46(13)
<i>Z</i>	4	4	2
<i>D</i> _{calcd} /g cm ⁻³	1.941	2.507	2.185
μ /mm ⁻¹	2.235	4.849	3.291
<i>R</i> indexes	<i>R</i> 1 = 0.0322, ^a [<i>I</i> > 2 σ (<i>I</i>)] <i>wR</i> 2 = 0.0929 ^b	<i>R</i> 1 = 0.0377, ^a <i>wR</i> 2 = 0.0726 ^b	<i>R</i> 1 = 0.0274, ^a <i>wR</i> 2 = 0.0605 ^b
<i>R</i> (all data)	<i>R</i> 1 = 0.0347, <i>wR</i> 2 = 0.0943	<i>R</i> 1 = 0.0596, <i>wR</i> 2 = 0.0808	<i>R</i> 1 = 0.0301, <i>wR</i> 2 = 0.0617

^a *R*1 = $\sum ||F_o| - |F_c|| / \sum |F_o|$. ^b *wR*2 = $\{\sum [w(F_o^2 - F_c^2)^2] / \sum [w(F_o^2)^2]\}^{1/2}$. $w = 1/[\sigma^2(F_o)^2 + (aP)^2 + bP]$, $P = [\max(F_o^2, 0) + 2(F_c^2)^2]/3$, where $a = 0.0489$ and $b = 2.8965$ for **I**, $a = 0.0191$ and $b = 7.0687$ for **II**, and $a = 0.0$ and $b = 0.0$ for **III**.

as absorption by the glass fiber, were simultaneously corrected. The structures were solved by direct methods, and, in each case, a sufficient fragment of the structure was revealed (Zn, P, and O) to enable the remainder of the non-hydrogen atoms to be located from difference Fourier maps and the refinements to proceed to *R* < 10%. One of the carbon atoms [C(2)] of the amine molecule in **I** was found to be disordered. The water molecule in **I** has a refined occupancy of ~ 0.46 . All of the hydrogen positions for **I–III** were initially located in the difference map, and for the final refinement the hydrogen atoms were placed geometrically and held in the riding mode, except for **I** where due to the disorder to the carbon atoms only part of the hydrogen atoms of the amine have been placed. The Flack polarity parameter⁴⁹ was optimized to establish the absolute structure for **III**. A refined value of 0.017(13) indicated that the absolute structure is as given in the Results. Setting the Flack parameter to 1.00 (opposite absolute structure) and repeating the refinement gave a refined value of 0.915(2). The last cycles of refinement included atomic positions for all of the atoms, anisotropic thermal parameters for all of the non-hydrogen atoms, and isotropic thermal parameters for all of the hydrogen atoms. Full-matrix least-squares refinement against $|F^2|$ was carried out using the SHELXTL-PLUS⁵⁰ suite of programs. Details of the final refinement are given in Table 1. The selected bond distances and angles are given in Table 2 for **I**, in Table 3 for **II**, and in Table 4 for **III**.

Results

Structure of the One-Dimensional Zinc Phosphate, [C₅N₂H₁₄][Zn(HPO₄)₂] \cdot *x*H₂O ($x = \sim 0.46$), **I.** The asymmetric unit of **I** contains 19 non-hydrogen atoms, of which 11 atoms belong to the zinc phosphate chain, seven atoms belong to the organic amine guest, and one atom belongs to the water molecule as shown in Figure 1. There are one Zn and two P atoms that are independent in the asymmetric unit. The Zn atom is tetrahedrally coordinated by four oxygen atoms with an average Zn–O distance of 1.953 Å. This value

(49) Flack, H. D. *Acta Crystallogr.* **1983**, A39, 876.

(50) Sheldrick, G. M. *SHELX-97 A program for crystal structure solution and refinement*; University of Göttingen: Göttingen, Germany, 1997.

(48) Sheldrick, G. M. *SADABS Siemens area detector absorption correction program*; University of Göttingen: Göttingen, Germany 1994.

Table 2. Selected Bond Distances and Angles for $[\text{C}_5\text{N}_2\text{H}_{14}][\text{Zn}(\text{HPO}_4)_2] \cdot x\text{H}_2\text{O}$ ($x \approx 0.46$), **I**^a

bond	distance (Å)	bond	distance (Å)
Zn(1)–O(1)	1.947(3)	P(1)–O(4)	1.532(3)
Zn(1)–O(2)	1.972(3)	P(1)–O(7)	1.585(3)
Zn(1)–O(3)	1.950(3)	P(2)–O(6)	1.518(3)
Zn(1)–O(4)	1.941(3)	P(2)–O(3)#1	1.519(3)
P(1)–O(1)#2	1.519(3)	P(2)–O(2)	1.530(3)
P(1)–O(8)	1.522(3)	P(2)–O(5)	1.579(3)
moiety	angle (deg)	moiety	angle (deg)
O(4)–Zn(1)–O(1)	113.69(12)	O(4)–P(1)–O(7)	105.29(17)
O(4)–Zn(1)–O(3)	115.11(13)	O(6)–P(2)–O(3)#1	112.13(17)
O(1)–Zn(1)–O(3)	107.56(12)	O(6)–P(2)–O(2)	109.66(17)
O(4)–Zn(1)–O(2)	113.07(12)	O(3)#1–P(2)–O(2)	113.13(17)
O(1)–Zn(1)–O(2)	105.31(12)	O(6)–P(2)–O(5)	107.77(19)
O(3)–Zn(1)–O(2)	100.91(13)	O(3)#1–P(2)–O(5)	108.11(17)
O(1)#2–P(1)–O(8)	113.91(17)	O(2)–P(2)–O(5)	105.69(18)
O(1)#2–P(1)–O(4)	112.60(17)	P(1)#2–O(1)–Zn(1)	126.96(17)
O(8)–P(1)–O(4)	110.04(17)	P(2)–O(2)–Zn(1)	131.37(18)
O(1)#2–P(1)–O(7)	108.51(16)	P(2)#1–O(3)–Zn(1)	130.67(18)
O(8)–P(1)–O(7)	105.89(18)	P(1)–O(4)–Zn(1)	122.36(17)

^a Symmetry transformations used to generate equivalent atoms: #1 $-x, -y + 1, -z + 1$; #2 $-x + 1, -y + 1, -z + 1$.

Table 3. Selected Bond Distances and Angles for $[\text{C}_5\text{N}_2\text{H}_{14}][\text{Zn}_3(\text{H}_2\text{O})(\text{PO}_4)_2(\text{HPO}_4)]$, **II**^a

bond	distance (Å)	bond	distance (Å)
Zn(1)–O(2)	1.909(4)	P(1)–O(3)#1	1.516(4)
Zn(1)–O(1)	1.940(4)	P(1)–O(6)#1	1.529(5)
Zn(1)–O(3)	1.941(4)	P(1)–O(9)	1.530(5)
Zn(1)–O(4)	2.027(4)	P(1)–O(4)	1.563(4)
Zn(2)–O(5)	1.905(4)	P(2)–O(12)	1.516(4)
Zn(2)–O(7)	1.952(4)	P(2)–O(2)	1.521(5)
Zn(2)–O(6)	1.978(4)	P(2)–O(1)#1	1.539(5)
Zn(2)–O(4)	2.015(4)	P(2)–O(13)	1.579(4)
Zn(3)–O(8)	1.898(4)	P(3)–O(5)#2	1.525(5)
Zn(3)–O(10)	1.943(4)	P(3)–O(8)#3	1.531(5)
Zn(3)–O(9)	1.946(4)	P(3)–O(7)#3	1.536(4)
Zn(3)–O(11)	1.984(4)	P(3)–O(10)	1.555(4)
moiety	angle (deg)	moiety	angle (deg)
O(2)–Zn(1)–O(1)	104.74(19)	O(12)–P(2)–O(2)	114.4(3)
O(2)–Zn(1)–O(3)	106.68(19)	O(12)–P(2)–O(1)#1	111.0(3)
O(1)–Zn(1)–O(3)	118.56(19)	O(2)–P(2)–O(1)#1	110.3(3)
O(2)–Zn(1)–O(4)	117.03(18)	O(12)–P(2)–O(13)	108.3(2)
O(1)–Zn(1)–O(4)	107.51(18)	O(2)–P(2)–O(13)	107.7(2)
O(3)–Zn(1)–O(4)	102.98(18)	O(1)#1–P(2)–O(13)	104.5(3)
O(5)–Zn(2)–O(7)	107.46(19)	O(5)#2–P(3)–O(8)#3	110.0(3)
O(5)–Zn(2)–O(6)	104.8(2)	O(5)#2–P(3)–O(7)#3	112.2(3)
O(7)–Zn(2)–O(6)	101.09(19)	O(8)#3–P(3)–O(7)#3	110.9(3)
O(5)–Zn(2)–O(4)	129.20(18)	O(5)#2–P(3)–O(10)	107.4(3)
O(7)–Zn(2)–O(4)	106.59(19)	O(8)#3–P(3)–O(10)	110.4(3)
O(6)–Zn(2)–O(4)	104.31(17)	O(7)#3–P(3)–O(10)	105.8(2)
O(8)–Zn(3)–O(10)	112.36(19)	P(2)#4–O(1)–Zn(1)	130.8(3)
O(8)–Zn(3)–O(9)	124.52(19)	P(2)–O(2)–Zn(1)	128.1(3)
O(10)–Zn(3)–O(9)	110.62(18)	P(1)#4–O(3)–Zn(1)	128.5(3)
O(8)–Zn(3)–O(11)	108.6(2)	P(1)–O(4)–Zn(2)	108.9(2)
O(10)–Zn(3)–O(11)	96.69(19)	P(1)–O(4)–Zn(1)	130.7(3)
O(9)–Zn(3)–O(11)	99.4(2)	P(3)#5–O(5)–Zn(2)	146.5(3)
O(3)#1–P(1)–O(6)#1	112.4(3)	P(1)#4–O(6)–Zn(2)	132.9(3)
O(3)#1–P(1)–O(9)	109.5(2)	P(3)#3–O(7)–Zn(2)	129.0(3)
O(6)#1–P(1)–O(9)	108.9(3)	P(3)#3–O(8)–Zn(3)	136.1(3)
O(3)#1–P(1)–O(4)	110.4(2)	P(1)–O(9)–Zn(3)	129.3(3)
O(6)#1–P(1)–O(4)	105.5(3)	P(3)–O(10)–Zn(3)	127.0(3)
O(9)–P(1)–O(4)	110.2(2)		

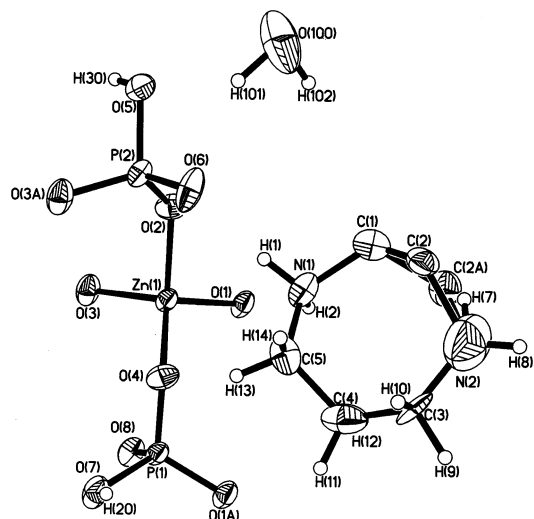
^a Symmetry transformations used to generate equivalent atoms: #1 $x, -y + 3/2, z + 1/2$; #2 $-x, y + 1/2, -z + 1/2$; #3 $-x, -y + 2, -z$; #4 $x, -y + 3/2, z - 1/2$; #5 $-x, y - 1/2, -z + 1/2$.

is comparable to values in other one-dimensional zinc phosphate compounds such as the ladder, $[\text{NH}_3(\text{CH}_2)_3\text{NH}_3]$ -

Table 4. Selected Bond Distances and Angles for $[\text{C}_5\text{N}_2\text{H}_{14}][\text{Zn}_2(\text{HPO}_4)_3] \cdot \text{H}_2\text{O}$, **III**^a

bond	distance (Å)	bond	distance (Å)
Zn(1)–O(2)	1.922(4)	P(1)–O(3)	1.523(4)
Zn(1)–O(4)	1.942(4)	P(1)–O(9)	1.586(4)
Zn(1)–O(3)	1.958(4)	P(2)–O(7)	1.511(4)
Zn(1)–O(1)	1.968(4)	P(2)–O(2)#2	1.517(5)
Zn(2)–O(6)	1.931(4)	P(2)–O(10)	1.523(4)
Zn(2)–O(5)	1.942(4)	P(2)–O(11)	1.588(4)
Zn(2)–O(7)	1.952(4)	P(3)–O(4)	1.515(4)
Zn(2)–O(8)	1.969(4)	P(3)–O(1)#3	1.539(4)
P(1)–O(6)	1.514(4)	P(3)–O(5)#3	1.539(4)
P(1)–O(8)#1	1.523(4)	P(3)–O(12)	1.575(4)
moiety	angle (deg)	moiety	angle (deg)
O(2)–Zn(1)–O(4)	117.76(17)	O(7)–P(2)–O(10)	111.6(2)
O(2)–Zn(1)–O(3)	109.95(17)	O(2)#2–P(2)–O(10)	111.4(2)
O(4)–Zn(1)–O(3)	100.17(16)	O(7)–P(2)–O(11)	105.0(2)
O(2)–Zn(1)–O(1)	112.93(17)	O(2)#2–P(2)–O(11)	108.4(3)
O(4)–Zn(1)–O(1)	100.73(16)	O(10)–P(2)–O(11)	108.5(2)
O(3)–Zn(1)–O(1)	114.63(16)	O(4)–P(3)–O(1)#3	112.1(2)
O(6)–Zn(2)–O(5)	114.36(18)	O(4)–P(3)–O(5)#3	109.3(2)
O(6)–Zn(2)–O(7)	109.37(17)	O(1)#3–P(3)–O(5)#3	111.6(2)
O(5)–Zn(2)–O(7)	114.87(17)	O(4)–P(3)–O(12)	107.3(2)
O(6)–Zn(2)–O(8)	113.03(16)	O(1)#3–P(3)–O(12)	106.9(2)
O(5)–Zn(2)–O(8)	104.91(16)	O(5)#3–P(3)–O(12)	109.5(2)
O(7)–Zn(2)–O(8)	99.29(16)	P(3)#4–O(1)–Zn(1)	133.0(2)
O(6)–P(1)–O(8)#1	108.7(2)	P(2)#5–O(2)–Zn(1)	135.3(3)
O(6)–P(1)–O(3)	112.8(2)	P(1)–O(3)–Zn(1)	132.2(2)
O(8)#1–P(1)–O(3)	112.7(2)	P(3)–O(4)–Zn(1)	150.8(3)
O(6)–P(1)–O(9)	111.3(2)	P(3)#4–O(5)–Zn(2)	132.2(2)
O(8)#1–P(1)–O(9)	104.7(2)	P(1)–O(6)–Zn(2)	128.8(2)
O(3)–P(1)–O(9)	106.4(2)	P(2)–O(7)–Zn(2)	139.9(3)
O(7)–P(2)–O(2)#2	111.7(2)	P(1)#6–O(8)–Zn(2)	133.1(2)

^a Symmetry transformations used to generate equivalent atoms: #1 $-x + 1, y + 1/2, -z$; #2 $x + 1, y, z$; #3 $-x + 1, y + 1/2, -z + 1$; #4 $-x + 1, y - 1/2, -z + 1$; #5 $x - 1, y, z$; #6 $-x + 1, y - 1/2, -z$.

**Figure 1.** ORTEP plot of **I**, $[\text{C}_5\text{N}_2\text{H}_{14}][\text{Zn}(\text{HPO}_4)_2] \cdot x\text{H}_2\text{O}$ ($x \approx 0.46$), showing the asymmetric unit. Thermal ellipsoids are given at 50% probability.

$[\text{Zn}(\text{HPO}_4)_2]$, $(\text{Zn}-\text{O})_{\text{av}} = 1.944 \text{ \AA}$.¹⁵ The O–Zn–O bond angles have an average value of 109.3° . The Zn atom is connected to two P atoms via four Zn–O–P linkages with an average angle of 127.8° . The phosphorus atoms, on the other hand, make only two P–O–Zn bonds and possess two terminal P–O linkages. The P–O distances are in the range $1.518(2)$ – $1.584(1) \text{ \AA}$ and have an average value of 1.537 \AA . The O–P–O bond angles are in the range $105.3(1)$ –

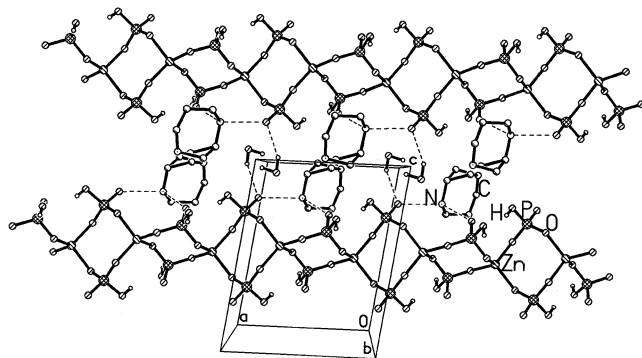


Figure 2. Structure of **I** in the *ac* plane showing the one-dimensional chain architecture. The amine and the water molecules occupy the interchain spaces. Dotted lines represent possible hydrogen bond interactions.

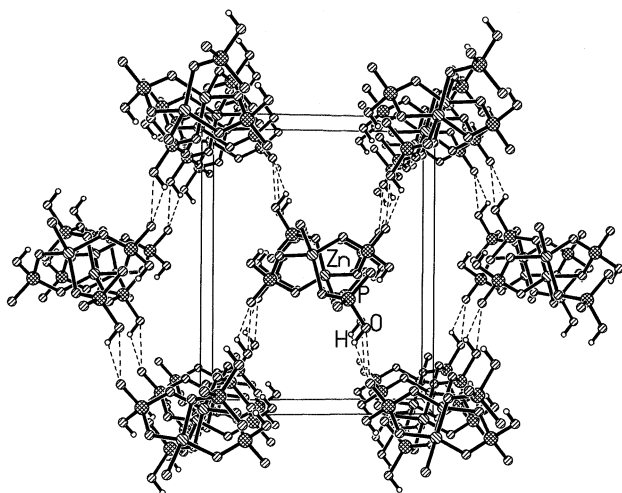


Figure 3. Structure of **I** along the chain axis. Note that four different chains form a channel-like structure through hydrogen bonds (see text). Dotted lines represent the various hydrogen bond interactions.

$115.1(1)^\circ$ [$\text{O}-\text{P}-\text{O}$]_{av} = 109.4°]. The P–O distances of P(1)–O(7) = 1.585(3) Å and P(2)–O(5) = 1.579(3) Å suggest that the oxygen atoms are protonated (Table 2). The presence of hydroxyl groups was confirmed by the observation of peaks corresponding to hydrogen positions close to these oxygen atoms, in the difference Fourier maps. The various P–O distances and O–P–O angles in **I** are consistent with those reported for similar compounds in the literature.^{2–40} Bond valence sum calculations⁵¹ also agree with the above assignments.

The strictly alternating ZnO₄ and HPO₄ tetrahedral units in **I** form S4Rs, which are linked through their corners forming the one-dimensional chains as shown in Figure 2. The individual chain units are held together by strong hydrogen bond interactions involving the amine and water molecules. Similar zinc phosphate chain arrangements have been observed before.¹² The one-dimensional chains also interact with each other through the terminal P–OH linkages forming cavities (Figure 3). The cavities resemble those observed in the organic channel structures formed through noncovalent interactions.⁵² The various hydrogen bond interactions in **I** are listed in Table 5.

Table 5. Important Hydrogen Bond Interactions in [C₅N₂H₁₄][Zn(HPO₄)₂] \cdot *x*H₂O (*x* = ~0.46), **I**, [C₅N₂H₁₄][Zn₃(H₂O)(PO₄)₂(HPO₄)], **II**, and [C₅N₂H₁₄][Zn₂(HPO₄)₃] \cdot H₂O, **III**

D–H \cdots A moiety	D–H (Å)	H \cdots A (Å)	D \cdots A (Å)	D–H \cdots A (deg)
Compound I				
N(1)–H(1) \cdots O(6)	0.90	1.86	2.722(3)	161
N(1)–H(2) \cdots O(8)	0.90	1.87	2.753(4)	167
C(3)–H(9) \cdots O(7)	0.97	1.88	2.816(1)	160
C(3)–H(10) \cdots O(2)	0.97	2.02	2.918(3)	154
C(5)–H(14) \cdots O(1)	0.97	2.56	3.507(2)	166
Compound II				
N(2)–H(9) \cdots O(12)	0.90	1.87	2.745(7)	164
N(2)–H(10) \cdots O(9)	0.90	2.07	2.911(7)	155
O(11)–H(20) \cdots O(1) ^a	0.99	1.63	2.600(7)	168
O(11)–H(30) \cdots O(12) ^a	0.99	1.63	2.612(6)	171
O(13)–H(50) \cdots O(10) ^a	0.82	2.03	2.710(6)	141
C(1)–H(3) \cdots O(6)	0.97	1.83	2.785(7)	167
C(1)–H(4) \cdots O(7)	0.97	2.01	2.825(7)	141
C(3)–H(8) \cdots O(11)	0.97	2.41	3.204(9)	139
C(5)–H(14) \cdots O(10)	0.97	2.56	3.505(4)	164
Compound III				
N(1)–H(1) \cdots O(5)	0.90	2.13	2.997(7)	161
N(1)–H(2) \cdots O(1)	0.90	2.02	2.914(6)	170
N(2)–H(9) \cdots O(8)	0.90	1.90	2.790(6)	173
N(2)–H(10) \cdots O(100)	0.90	1.92	2.786(7)	162
O(12)–H(20) \cdots O(10) ^a	0.82	1.68	2.474(6)	162
O(11)–H(30) \cdots O(12) ^a	0.82	1.86	2.670(6)	170
O(9)–H(40) \cdots O(11) ^a	0.82	1.95	2.723(6)	157
O(100)–H(101) \cdots O(3)	0.99	1.87	2.831(6)	163
O(100)–H(102) \cdots O(10)	0.99	1.75	2.693(7)	158
C(1)–H(4) \cdots O(9)	0.97	2.58	3.476(7)	154
C(3)–H(7) \cdots O(9)	0.97	2.48	3.336(8)	147

^a Intraframework interactions.

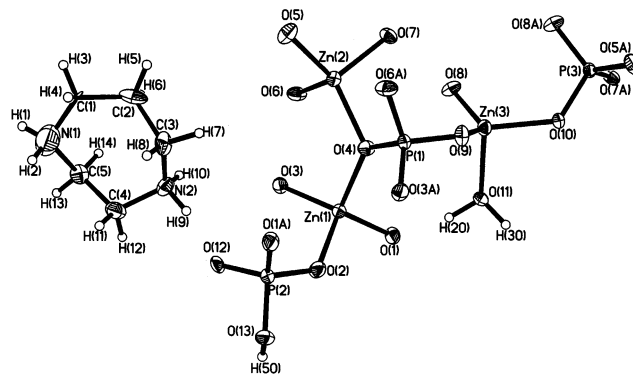


Figure 4. ORTEP plot of **II**, [C₅N₂H₁₄][Zn₃(H₂O)(PO₄)₂(HPO₄)], showing the asymmetric unit. Thermal ellipsoids are given at 50% probability.

Structure of the Two-Dimensional Zinc Phosphate, [C₅N₂H₁₄][Zn₃(H₂O)(PO₄)₂(HPO₄)], **II.** The asymmetric unit of **II** contains 26 non-hydrogen atoms, of which 19 belong to the framework and seven belong to the guest amine molecule (Figure 4). There are three crystallographically distinct Zn and P atoms. The Zn atoms are tetrahedrally coordinated by their O atom neighbors with Zn–O bond lengths in the range 1.898(4)–2.027(5) Å (average Zn(1)–O = 1.954 Å, Zn(2)–O = 1.963 Å, Zn(3)–O = 1.993 Å). The O–Zn–O bond angles are in the range 96.7(1)–129.2(2)° (average O–Zn(1)–O = 109.6°, O–Zn(2)–O = 108.9°, O–Zn(3)–O = 108.7°). Of the three zinc atoms, Zn(1) and

(51) Brown, I. D.; Altermatt, D. *Acta Crystallogr., Sect. B* **1985**, *41*, 244.

(52) Pedireddi, V. R.; Chatterjee, S.; Ranganathan, A.; Rao, C. N. R. *J. Am. Chem. Soc.* **1997**, *119*, 10867 and the references therein.

Zn(2) make four Zn–O–P bonds, while Zn(3) makes only three such bonds and possesses one terminal Zn–O linkage, resulting in an average Zn–O–P angle of 129.8° . Similarly P(2) makes only three P–O–Zn bonds with one terminal P–O bond, and P(1) and P(3) make four P–O–Zn bonds. The P–O distances are in the range $1.516(4)$ – $1.579(4)$ Å (average 1.537 Å), and the O–P–O angles are in the range $104.5(3)$ – $112.4(3)^\circ$ (average 109.4°). These geometrical parameters are in good agreement with those reported for similar compounds in the literature.^{2–40} The framework structure of $\text{Zn}_3\text{O}(\text{PO}_4)_3$ would result in a net framework charge of -5 . The presence of one H-PIP would account for a $+2$ charge, arising from the complete protonation of the amine molecule. The excess negative charge of -3 is then needed to be balanced. Bond valence calculations⁵¹ indicate that P(2)–O(13) with a distance of $1.579(4)$ Å is formally a OH group and Zn(3)–O(11) with a distance of 1.984 Å is a water molecule, which, incidentally, also corresponds well with the proton positions located in the difference Fourier maps. The other larger distances, Zn(1)–O(4) = $2.027(4)$ Å, Zn(2)–O(4) = $2.015(4)$ Å, and P(1)–O(4) = $1.563(4)$ Å, are associated with a three-coordinated oxygen atom, O(4). Formation of terminal water molecules linked to Zn centers has been known to occur in open-framework three-dimensional zinc phosphates.³⁸ This is the first observation, to our knowledge, of such a terminal water molecule in a two-dimensional layered structure. The selected bond distances and angles are listed in Table 3.

The framework structure of **II** consists of ZnO_4 , PO_4 , and $\text{PO}_3(\text{OH})$ tetrahedral units linked through their vertices. The connectivity between these units gives rise to an unusual layer architecture as shown in Figure 5. The layers can be understood in terms of the one-dimensional corner-shared chains. Thus, Zn(1) \times 2, P(1), and P(2) tetrahedral units, and Zn(2) \times 2, P(1), and P(3) tetrahedral units form two independent one-dimensional corner-shared chains. These two chain units are connected (fused) through the 3-coordinated oxygen atom, O(4), to give rise to a strip-like arrangement (Figure 5a). These strips are joined together by Zn(3)O₄ tetrahedra giving rise to a layer structure with an eight-membered bifurcated aperture. The connectivity between the strip and Zn(3) tetrahedra is such that it forms a tube-like arrangement within the layer. This is indeed an unusual arrangement for a two-dimensional zinc phosphate layer. The layer arrangement along the *ab* plane is shown in Figure 6. As can be seen, the layer arrangement is in AAAA fashion. Looking down the strip or tube, we see that the strip is connected by four-membered rings, which are arranged to give a sinusoidal character to the layer arrangement. This connectivity of the tubes and their positions with respect to the adjacent layers is reminiscent of the lock and key arrangement, observed commonly in enzymes. The amine molecule occupies the interlamellar region and interacts with the framework through strong N–H \cdots O and C–H \cdots O hydrogen bonds. In addition, the terminal water molecule from the Zn center also participates in hydrogen bonds. The complete list of hydrogen bond interactions in **II** is listed in Table 5.

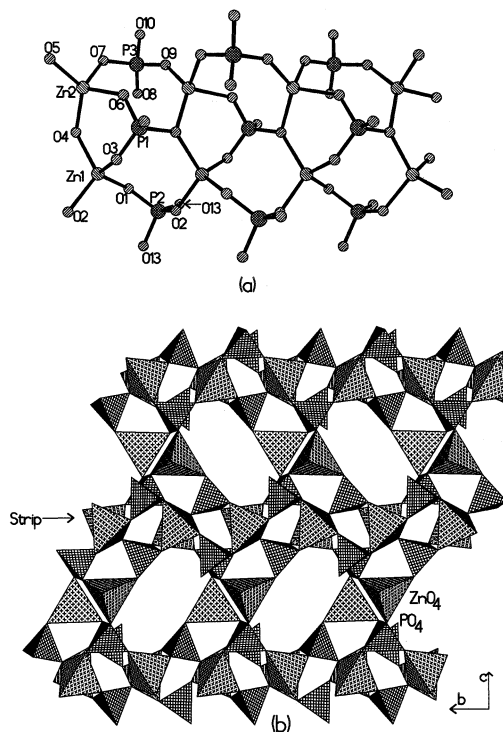


Figure 5. (a) Structure of **II** showing the strip-like arrangement formed between two independent corner-shared chains connected through the 3-coordinated oxygen atoms. (b) Polyhedral representation of **II** showing a single layer. The strip-like feature is marked by the arrow.

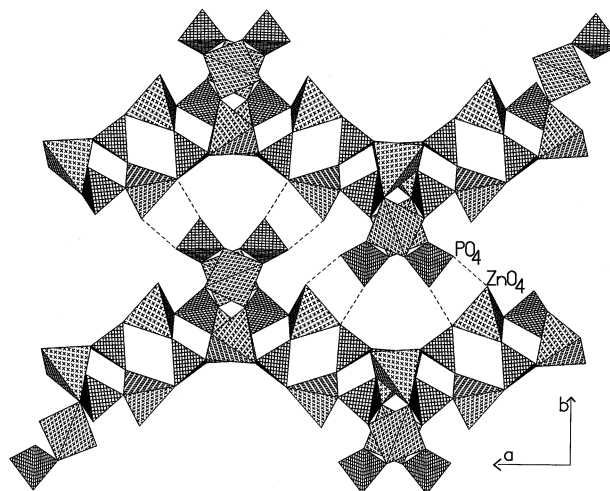


Figure 6. Polyhedral view of the structure of **II** in the *ab* plane showing the arrangement of layers. The amine molecules are not shown for clarity. Dotted lines represent possible hydrogen bond interactions between the layers (See Table 5). Note that the tube-like arrangement is connected by four-membered rings and the positioning of two adjacent layers resembling the lock and key type arrangement.

Structure of the Three-Dimensional Zinc Phosphate, $[\text{C}_5\text{N}_2\text{H}_{14}][\text{Zn}_2(\text{HPO}_4)_3]\cdot\text{H}_2\text{O}$, **III.** The asymmetric unit of **III** contains 25 non-hydrogen atoms (Figure 7), of which 17 atoms belong to the framework, seven atoms to H-PIP, and one atom belongs to the water molecule. There are two crystallographically distinct Zn atoms and three P atoms. The structure is essentially constructed from the strictly alternating vertex linkage of ZnO_4 and HPO_4 tetrahedra forming macroanionic layers. The Zn atoms are all tetrahedrally coordinated to four oxygen atoms. The Zn–O distances are

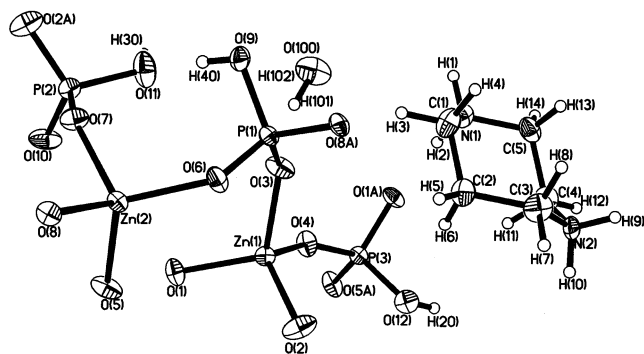


Figure 7. ORTEP plot of **III**, $[\text{C}_5\text{N}_2\text{H}_{14}][\text{Zn}_2(\text{HPO}_4)_3]\cdot\text{H}_2\text{O}$, showing the asymmetric unit. Thermal ellipsoids are given at 50% probability.

in the range 1.922(4)–1.969(4) Å (average Zn–O = 1.947 Å), and the O–Zn–O angles are in the range 99.3(2)–117.7(2)° (average O–Zn–O = 109.4° for all of the Zn atoms). Both the Zn atoms are connected to three neighboring P atoms via four Zn–O–P bonds with an average bond angle of 135.7°. Of the three P atoms, P(1) and P(3) make three P–O–Zn bonds and possess one P–O terminal linkage, while P(2) makes two P–O–Zn linkages and has two P–O terminal bonds. The three P atoms have P–O distances in the range 1.511(4)–1.588(4) Å (average P–O = 1.538 Å), and the O–P–O angles are in the range 104.7(2)–112.8(2)° (average O–P–O = 109.4° for all of the P atoms). These geometrical parameters are in good agreement with those observed earlier.^{2–40} Assuming the usual valences of Zn, P, and O to be +2, +5, and –2, respectively, the framework stoichiometry of $\text{Zn}_2(\text{PO}_4)_3$ creates a net framework charge of –5. Taking into account the presence of $[\text{C}_5\text{N}_2\text{H}_{14}]^{2+}$, the excess negative charge of –3 can be balanced by the protonation of the PO_4 tetrahedra. One hydrogen position for each of the oxygen atoms, O(9), O(11), and O(12), has been observed in the difference Fourier maps. Thus, P(1)–O(9), P(2)–O(11), and P(3)–O(12) with distances of 1.586(4), 1.588(4), and 1.575(4) Å, respectively, are all P–OH units. The second terminal P–O linkage, in the case of P(2) with a P–O distance of 1.523(4) Å, is a P=O unit. This assignment is also consistent with bond valence sum calculations.⁵¹ The selected bond distances and angles are presented in Table 4.

The structure of **III** is constructed exclusively by ZnO_4 and $\text{PO}_3(\text{OH})$ tetrahedral units connected through their vertices. The structure can be thought of as consisting of two parts. The first is a zeolite-related layer made up of $\text{Zn}_2\text{P}_2\text{O}_8$ S4Rs, formed by $\text{Zn}(1)\text{O}_4$, $\text{Zn}(2)\text{O}_4$, $\text{P}(1)\text{O}_3(\text{OH})$, and $\text{P}(3)\text{O}_3(\text{OH})$ tetrahedral units. These S4Rs are linked together to form a layer that contains eight-ring windows. When viewed in the bc direction (Figure 8), the structure closely resembles that of the zeolite ABW,⁴⁶ which is composed of eight-rings linked by four-rings. This topology has also been observed for a number of other zeolites and zeolite analogues.⁴⁷ These zeolite-like layers are connected into a three-dimensional structure by cross-linking of P(2)–O₃(OH) tetrahedra. The overall structure consists of a three-dimensional framework with interconnecting eight-ring channels formed by the linking of the layers, producing pores

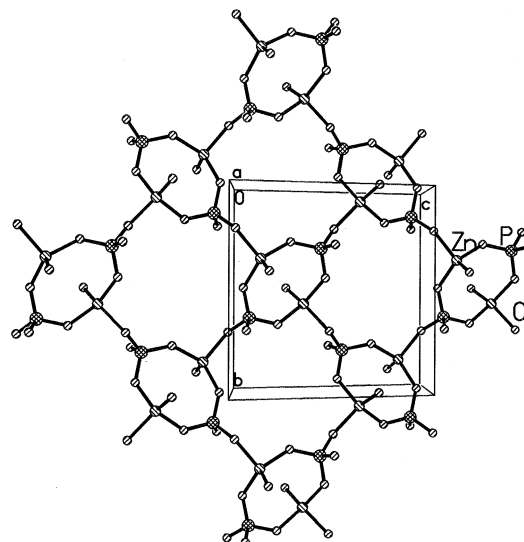


Figure 8. Structure of **III** in the bc plane showing the zeolite-like layers. These layers are connected by phosphate tetrahedral units forming one-dimensional channels (see text).

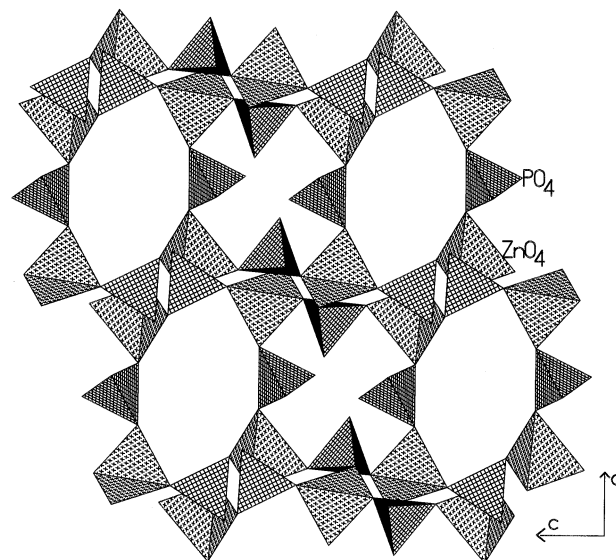


Figure 9. Polyhedral view of the structure of **III** in the ac plane showing the two types of eight-membered channels. The narrower channels are hydrophilic, and the larger elliptical channels are hydrophobic (see text).

that run parallel to the plane of the layers, and by the zeolitic nature of the layers themselves, which stack on top of each other to form channels perpendicular to the plane of the layers. The connectivity between the layers in the ab plane gives rise to two types of channels bound by eight T (T = Zn, P) atoms as shown in Figure 9. What is interesting about this channel structure is that the channels have alternate hydrophobic and hydrophilic nature, with the water molecule occupying the hydrophilic channel and the organic amine molecule the hydrophobic channel, respectively. Along the ab plane, the linkages between Zn(1), Zn(2), P(1), and P(3) tetrahedra are aligned along the 2-fold screw axis and are connected by P(2) tetrahedra to give rise to irregular 10-membered channels as shown in Figure 10. The doubly protonated H-PIP molecule sits in the channels along with one water molecule and interacts with the framework through

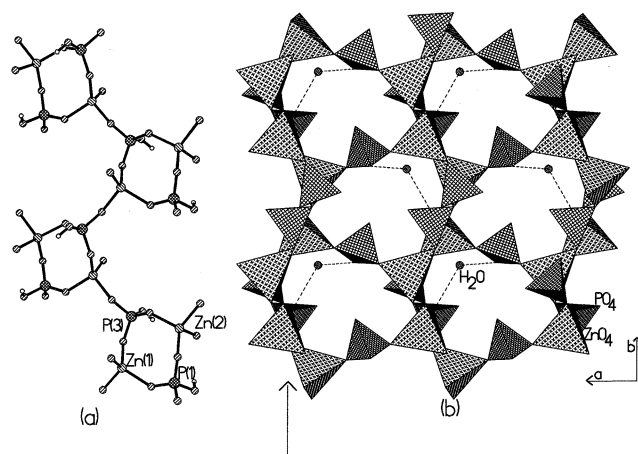


Figure 10. (a) The connectivity between the four-membered rings along the 2-fold screw axis. (b) Polyhedral view of the structure of **III** in the *ab* plane showing the irregular shaped channels. Water molecules are shown within the channels. Arrow indicates the direction of the screw axis. Amine molecules are not shown for clarity.

hydrogen bonds. The complete list of the hydrogen bond interactions in **III** is given in Table 5.

The “openness” of a structure is defined in terms of the tetrahedral atom density⁴⁷ (framework density, FD), defined as the number of tetrahedral (T) atoms per 1000 Å³. In **III**, the number of T atoms per 1000 Å³ (here T = Zn, P) is 12.2. This value shows a degree of openness comparable to that of many of the aluminosilicate zeolites and aluminophosphates.⁴⁷

Discussion

Three new zinc phosphates, [C₅N₂H₁₄][Zn(HPO₄)₂] \cdot *x*H₂O (*x* = ~0.46), **I**, [C₅N₂H₁₄][Zn₃(H₂O)(PO₄)₂(HPO₄)], **II**, and [C₅N₂H₁₄][Zn₂(HPO₄)₃] \cdot H₂O, **III**, have been obtained as good quality single crystals by hydrothermal methods, by employing minor variations in the synthesis mixture. The unpredictable nature of the kinetically controlled solvent-mediated reactions is well-illustrated by the formation of three different phases with varying dimensionality. As is typical of such reactions, there is no correlation between the starting composition and the majority solid-phase product.

The structures are formed from the expected tetrahedral building blocks of ZnO₄ and PO₄ units, sharing vertices, with linkages arising predominantly from Zn–O–P bonds. The one- and three-dimensional zinc phosphates (**I**–**III**) have a Zn:P ratio of >1.0, while the layered one (**II**) has a Zn/P ratio of 1.0. Layered zinc phosphates generally have a Zn:P ratio of >1.0.^{17–21} Layered zinc phosphate structure with a Zn/P ratio of 1.0 has only been observed recently.²⁰ Structurally, compound **I** is formed by corner-shared S4Rs, compound **II** is formed by the linkages involving two one-dimensional chains, made from S4Rs, joined via a 3-coordinate oxygen atom, and **III** is formed by S4Rs joined through oxygen atoms. The isolation of corner-shared zinc phosphate chain architectures, observed in **I**, is important, because the corner-shared chain structure is considered to be the primary building unit in one of the mechanisms proposed for the

formation of phosphates possessing open structures.⁴¹ In light of this, it is interesting to note that a similar one-dimensional chain unit is also present in **II**. The fundamental building unit, the S4R, Zn₂P₂O₈, made from two Zn and two P atoms connected by oxygen atoms, proposed by Rao et al.,^{37,38} is also present in all three compounds. The observed differences between the three structures are essentially due to the differences in their connectivity between the S4R units.

Multipoint hydrogen bond interactions play a subtle role in the formation and stability of open architectures. In **I**–**III**, we find such hydrogen bond interactions with short donor–acceptor distances (~2.7–3.0 Å) and donor–hydrogen–acceptor bond angles of >150°. The important hydrogen bond interactions are listed in Table 5.

The synthesis of more than one type of zinc phosphate structure with varying Zn:P ratio has been shown by Harrison et al.³¹ with guanidine as the amine. The amine of the nitrogen-rich guanidine cation, [C(NH₃)₃]⁺, was presumed to have a symmetrical, propeller shape. The use of linear triamines such as diethylenetriamine, DETA, on the other hand, also appears to be favorable for the formation of dissimilar structures.^{17,36} Use of linear diamines such as 1,3-diaminopropane gives rise to variety of structures with varying dimensionality.^{14,15,18,38} By employing a cyclic diamine, we have now obtained three different phosphates with one-, two-, and three-dimensional structures. Though the exact mechanism of formation of these architectures is far from being understood, it can be safely presumed that the nitrogen atoms of the amine molecule play a vital role.

The syntheses of **I**–**III** have been carried out by the addition of acetic acid in addition to hydrochloric acid. It is likely that the Cl[–] ions might just be acting as a mineralizer similar to the F[–] ions in some of the syntheses of the phosphates of Al and Ga.⁵³ The role of acetic acid is still not clear. It is likely that the acetate ions, present in the mixture during the synthesis, might act as a base and favor the deprotonation of H₃PO₄. While prediction of the overall structure of such complex organic–inorganic hybrid materials remains elusive, further studies are necessary to evaluate the interplay of structural subunits in the construction of solids and to understand the minor compositional variations in yielding different open-framework structures.

Acknowledgment. The author thanks Prof. C. N. R. Rao, FRS, for his support and encouragement. The author also thanks the Council of Scientific and Industrial Research (CSIR), Government of India, for the award of a research grant.

Supporting Information Available: Simulated and observed powder X-ray diffraction patterns for **I** and **II**. X-ray crystallographic files in CIF format for **I**–**III**. This material is available free of charge via the Internet at <http://pubs.acs.org>.

IC0203872

(53) Chippindale, A. M.; Natarajan, S.; Thomas, J. M.; Jones, R. H. *J. Solid State Chem.* **1994**, *111*, 18 and references therein.